

# Orientation Dependent Characteristics of Recessed-Gate InGaAs/AlGaAs HEMTs

Tomoyuki Ohshima, Masaaki Yoshida, Ryoji Shigemasa,  
Masanori Tsunotani and Tamotsu Kimura

III-V Devices Department, Components Division, Oki Electric Industry  
550-1 Higashiasakawa, Hachioji, Tokyo 193-8550, Japan  
Phone: +81-426-62-6669, Fax: +81-426-62-6616, e-mail: ohshima752@oki.co.jp

## ABSTRACT

The effect of the gate orientation for pseudomorphic InGaAs/AlGaAs HEMTs with recessed-gate structure has been investigated. The short channel effect strongly depends on the gate orientation and is significant in the order of [0-11], [001] and [0-1-1] oriented devices. Such orientation dependence results from a difference of the side-etching length affected by the crystal orientation. The electrical characteristics of HEMTs such  $BV_{gds}$ ,  $gm$  and  $f_T$  also depend on the gate orientation because of a difference of the recessed shape.

## INTRODUCTION

The pseudomorphic InGaAs/AlGaAs HEMTs have been developed for the application of high-speed optical fiber communication systems and millimeter-wave wireless communication systems [1][2]. In order to design such MMICs with more compact chip size, flexibility for various circuit layouts is required to semiconductor devices. However, the electrical characteristics of compound semiconductor FETs strongly depend on the gate orientation relative to the substrate. For the ion-implanted GaAs MESFET with a planar structure, the orientation dependent characteristic has been understood in terms of the piezoelectric effect [3]-[5]. On the other hand, the recessed shape depending on the crystal orientation could affect the electrical characteristic of HEMTs with recessed-gate structure [6]-[8].

The purpose of this study is to investigate the gate orientation dependence of InGaAs/AlGaAs HEMTs formed by the wet-chemical recess etching.

## EXPERIMENTAL

The single recessed-gate pseudomorphic  $In_{0.2}Ga_{0.8}As/Al_{0.28}Ga_{0.72}As$  HEMT was used in this study [9]. All the layers were grown by MBE. The recess etching was performed using citric acid based solution as an etchant to remove the 55-nm-thick GaAs cap layer. The selectivity of as high as 200 was obtained for GaAs on  $Al_{0.28}Ga_{0.72}As$  using

the etchant. After the recess etching, Al/Ti gate electrodes were evaporated and lifted off. The substrate was (100) GaAs with an orientation flat of (0-1-1) plane. Three types of HEMTs with the gate electrodes oriented along [0-1-1], [001] and [0-1-1] directions were formed as shown in Fig. 1.

## ORIENTATION DPENDENCE OF SHORT CHANNEL EFFECT

Figure 2 shows the dependence of the threshold voltage ( $V_{th}$ ) on the gate length ( $L_g$ ) of the HEMTs oriented along [0-1-1], [001] and [0-11] directions. As shown in Fig. 2, the  $V_{th}$  decreased as the  $L_g$  reduced due to the short channel effect. However it was found that the short channel effect strongly depends on the gate orientation and is more significant in the order of [0-11], [001] and [0-1-1] oriented devices. This is not due to the piezoelectric effect because the  $V_{th}$  did not change before and after the deposition of a 500-nm-thick  $Si_3N_4$  film with a high tensile stress of  $3 \times 10^9$  dyn/cm<sup>2</sup>. To investigate the reason for the orientation dependent characteristics of the HEMTs, a cross-sectional SEM analysis around the gate recess was performed. As shown in Fig. 3, the flat recessed bottoms were obtained for all the devices, which means that the vertical etching of the GaAs cap layer stopped precisely at the AlGaAs surface. However, the

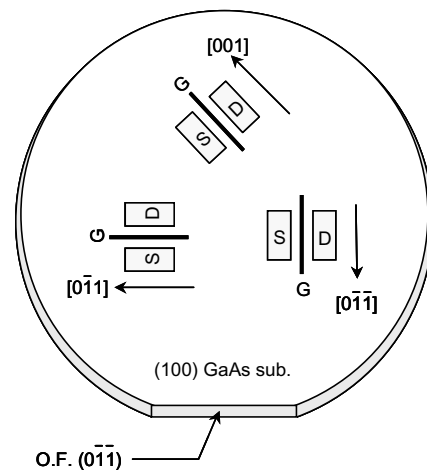


Fig. 1 Gate orientation relative to the (100) GaAs substrate.

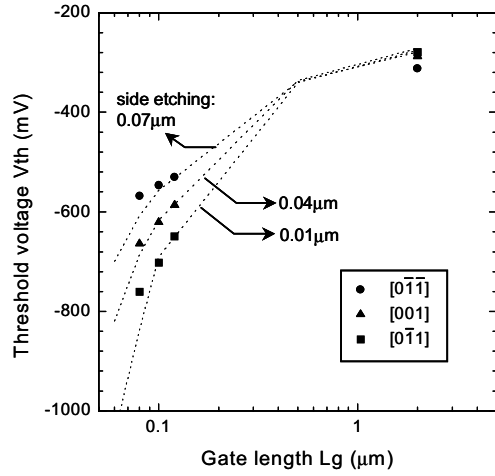


Fig. 2 Dependence of the threshold voltage on the gate length for the [0-1-1], [001] and [0-11] oriented devices. The dotted line shows the simulated result.

profiles of the recessed wall strongly depend on the gate orientation because of the dependence of the etching rate on the crystal orientation of GaAs [10]. From the viewpoint of the device characteristics, the most critical point in the recessed profiles could be the side-etching length, which is defined as the distance between the edge of the gate metal adjoining the substrate and the edge of the flat recessed bottom. The side-etching lengths obtained from Fig. 3 were larger in the order of [0-1-1], [001] and [0-11] oriented devices, and were 0.06, 0.03 and 0.01  $\mu\text{m}$ , respectively. In order to investigate the influence of the side-etching length on the HEMT characteristics, a two-dimensional device simulation was performed [11]. The recessed shape was simplified to a rectangular-shape with a constant depth and only the side-etching length was varied. The dependence of the calculated  $V_{th}$  on  $L_g$  is shown in Fig. 2 by dotted lines as a function of the side-etching length. As shown in Fig. 2, the orientation dependence of the short channel effect can be well explained by varying the side-etching length. The smaller side-etching length results in a larger short channel effect. The side-etching lengths of 0.07, 0.04 and 0.01  $\mu\text{m}$  fitted by the simulation agree well with the measured side-etching lengths of 0.06, 0.03, 0.01  $\mu\text{m}$  for the [0-1-1], [001] and [0-11] oriented devices, respectively in Fig. 3. Figure 4 shows the profiles of the electron concentration of the HEMTs with the side-etching lengths of 0.02  $\mu\text{m}$  and 0.10  $\mu\text{m}$ . The drain and the gate voltages are 2.0 V and 0 V, respectively. The depletion region under the gate is plotted as a dark area. As shown in Fig. 4, the depletion region spreads out under the recessed bottom. The effective gate area, under where the electron concentration within the

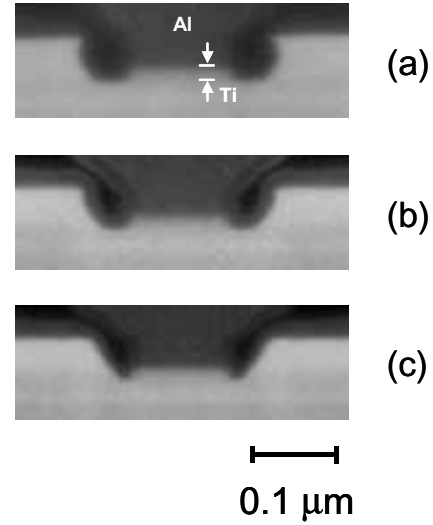


Fig. 3 SEM images of recessed region for the [0-1-1] (a), [001] (b) and [0-11] (c) oriented devices.

channel is modulated by gate bias, can be defined as the depleted layer width upon the channel [12]. Then, the effective gate length ( $L_{geff}$ ) was graphically obtained from the contour plot of the electron concentration at  $3 \times 10^{17} \text{ cm}^{-3}$ , which corresponds to a 10% of the donor concentration. Figure 5 shows the dependence of the effective gate length on the side-etching length. As shown in the figure, it was found that the effective gate length reduced as decreased the side-etching length. The shift of the threshold voltage for each device was summarized in Fig. 6 with respect to the effective gate length taking into account of the measured side-etching length. As shown in the figure, it is clear that the orientation dependent short channel effect for the recessed-gate HEMTs can be well explained by the effective gate length.

#### HEMT CHARACTERISTICS DEPENDING ON GATE ORIENTATION

The other characteristics of HEMTs depending on the gate orientation can also be understood in terms of the difference of the recessed shape. Figure 7 shows the transconductance ( $g_m$ ) and the gate to drain breakdown voltage ( $BV_{gd}$ ) for the HEMTs oriented along [0-1-1], [001] and [0-11] directions. By summarizing the data from the viewpoint of the side-etching length, it is clear that there exists a trade-off between  $g_m$  and  $BV_{gd}$ . As the side-etching length is increased,  $BV_{gd}$  increases due to a reduction of the maximum electric field strength at the drain side, while  $g_m$  decreases due to an increase of the source resistance. The RF performance of HEMTs also depends on the gate orientation. Figure 8

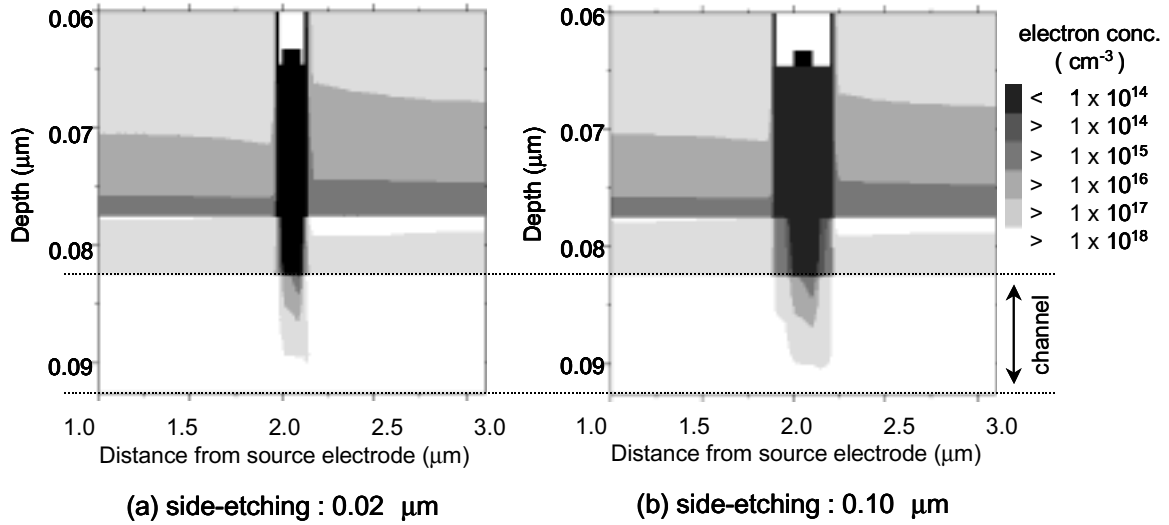


Fig. 4 Profiles of electron concentration for the HEMTs with the side-etching lengths of (a) 0.02  $\mu\text{m}$  and (b) 0.10  $\mu\text{m}$ .

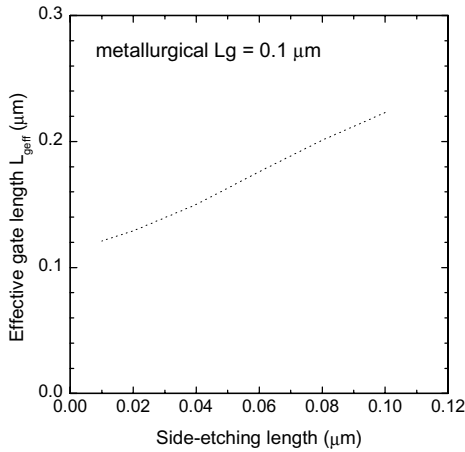


Fig. 5 Dependence of the effective gate length on the side-etching length.

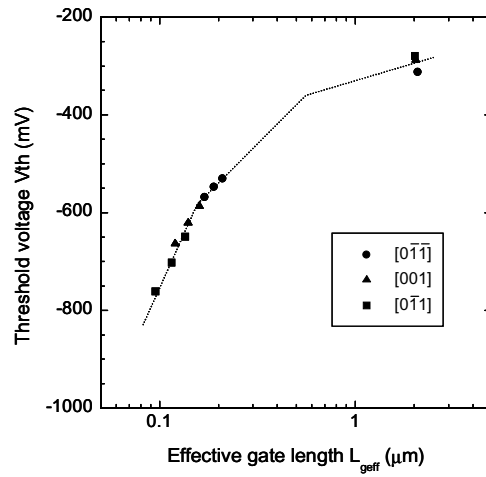


Fig. 6 Dependence of the threshold voltage on the effective gate length.

shows the current gain cut-off frequencies ( $f_T$ ) extracted from S-parameter measurements for the HEMTs of 100  $\mu\text{m}$ -width. As shown in Fig. 8,  $f_T$  increases in the order of [0-1-1], [001] and [0-11] oriented devices, which means that a small side-etching length results in a reduction of  $f_T$  in spite of an increase of  $g_m$ . Figure 8 also shows the gate capacitance ( $C_g$ ) obtained from a small signal equivalent circuit extraction by fitting the S-parameters. It was found that  $C_g$  increases as the side-etching length decreases. Since the distance between the footprint of the gate electrode and  $n^+$ -GaAs cap

layer decreases by reducing the side-etching length, the fringing gate capacitance increases and thus  $f_T$  degrades.

## CONCLUSIONS

The orientation dependence of the recessed-gate pseudomorphic InGaAs/AlGaAs HEMTs has been evaluated. It was found that the short channel effect was affected by the gate orientation relative to the substrate and was significant in

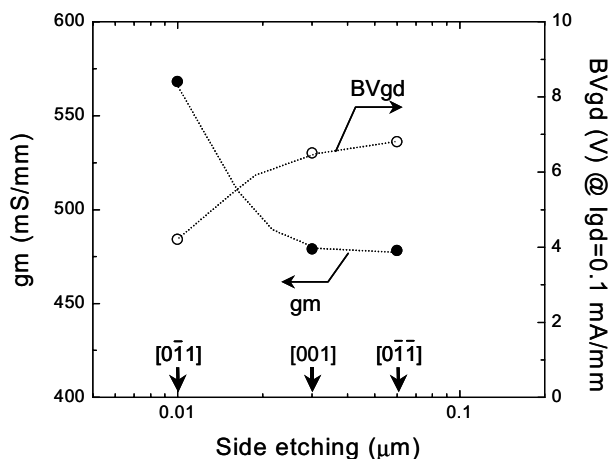


Fig. 7 Dependence of  $BV_{gd}$  and  $g_m$  on the side-etching length for the [0-1-1], [001] and [0-11] oriented devices.

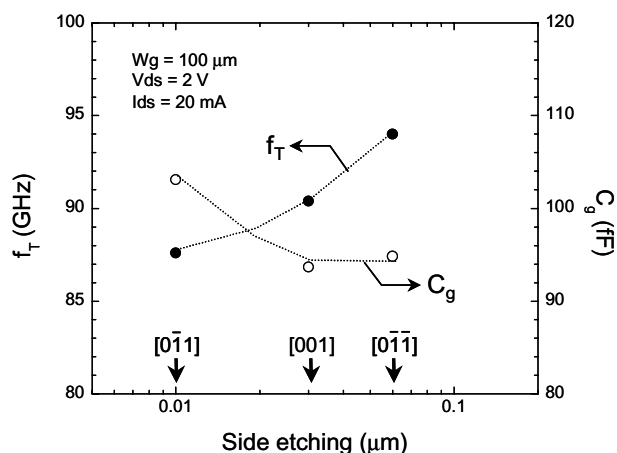


Fig. 8 Dependence of  $f_T$  and  $C_g$  on the side-etching length for the [0-1-1], [001] and [0-11] oriented devices.

the order of [0-11], [001] and [0-1-1] oriented devices. From a two dimensional device simulation, it was found that the orientation dependent short channel effect was explained by a difference of the side-etching length, which was affected by the crystal orientation. As increased the side-etching length, the effective gate length increased because the depletion layer, modulating the electron concentration in the channel, was expanding under the recessed bottom. The difference of the side-etching length also resulted in the orientation dependent characteristics of HEMTs such  $BV_{gd}$ ,  $g_m$  and  $f_T$ .

#### REFERENCES

- [1] H. Ikeda, T. Ohshima, M. Tsunotani, S. Seki and T. Kimura: *Tech. Dig. IEEE GaAs IC Symp., Seattle, 2000*, p.193
- [2] A. Nishino, T. Ohshima, M. Tsunotani, S. Seki and T. Kimura: *Tech. Dig. Optical Fiber Communication Conf., San Diego, 1999, WM-58-1*, p.365.
- [3] P. M. Asbeck, C. P. Lee and M. C. F. Chang: *IEEE Trans. Electron Devices* **31** (1984) 1377.
- [4] S. H. Lo and C. P. Lee: *IEEE Trans. Electron Devices* **37** (1990) 2130.
- [5] T. Kimura and T. Ohshima: *Jpn. J. Appl. Phys.* **32** (1993) 183.
- [6] G. C. DeSalvo, W. F. Tseng and J. Comas: *J. Electrochem. Soc.* **139** (1992) 831.
- [7] C. Juang, K. J. Kuhn and R. B. Darling: *J. Vac. Sci. & Technol. B* **8** (1990) 1122.
- [8] M. Tong, D. G. Ballegeer, A. Ketterson, E. J. Roan, K. Y. Cheng and I. Adesida: *J. Electron. Mater.* **21** (1992) 9.
- [9] T. Ohshima, R. Shigemasa, M. Sato, M. Tsunotani and T. Kimura: *Solid-State Electron.* **43** (1999) 1519.
- [10] M. Otsubo, T. Oda, H. Kumabe and H. Miki: *J. Electrochem. Soc.* **123** (1976) 676.
- [11] R. Anholt: *Electrical and Thermal Characterization of MESFETs, HEMTs and HBTs* (Artech, Norwood, 1995) Chap. 2.
- [12] T. Kimura and T. Ohshima: *Jpn. J. Appl. Phys.* **36** (1997) 5464.